Reaction of Glyoxal with 2‘-Deoxyguanosine, 2‘-Deoxyadenosine, 2‘-Deoxycytidine, Cytidine, Thymidine, and Calf Thymus DNA: Identification of DNA Adducts

ARTICLE *in* CHEMICAL RESEARCH IN TOXICOLOGY · MAY 2005

Impact Factor: 3.53 · DOI: 10.1021/tx0496688 · Source: PubMed

Reaction of Glyoxal with 2′-Deoxyguanosine, 2′-Deoxyadenosine, 2′-Deoxycytidine, Cytidine, Thymidine, and Calf Thymus DNA: Identification of DNA Adducts

Raymond Olsen,[†,‡] Paal Molander,[†,‡] Steinar Øvrebø,[†,§] Dag G. Ellingsen,[†] Syvert Thorud,[†] Yngvar Thomassen,[†] Elsa Lundanes,[‡] Tyge Greibrokk,[‡] Josefin Backman,[⊥] Rainer Sjöholm,[⊥] and Leif Kronberg*[,⊥]

National Institute of Occupational Health, P.O. Box 8149 Dep., N-0033 Oslo, Norway, Department of Chemistry, University of Oslo, P.O. Box 1033 Blindern, N-0315 Oslo, Norway, Department of Biology, University of Oslo, P.O. Box 1066 Blindern, N-0316 Oslo, Norway, and Department of Organic Chemistry, Åbo Akademi University, Biskopsgatan 8, FIN-20500 Åbo, Finland

Received December 1, 2004

Glyoxal (ethanedial) is an increasingly used industrial chemical that has been found to be mutagenic in bacteria and mammalian cells. In this study, the reactions of glyoxal with 2′-deoxyguanosine, 2′-deoxyadenosine, 2′-deoxycytidine, cytidine, thymidine, and calf thymus DNA have been studied in aqueous buffered solutions. The nucleoside adducts were isolated by reversed-phase liquid chromatography and characterized by their UV absorbance and ^{1}H and ^{13}C NMR spectroscopic and mass spectrometric features. The reaction with 2′-deoxyguanosine gave one adduct, the previously known 3-(2′-deoxy-β-D-*erythro*-pentofuranosyl)-5,6,7-trihydro-6,7-dihydroxyimidazo[1,2-*a*]purine-9-one adduct. The reaction of 2′-deoxyadenosine with glyoxal resulted in the formation of a previously not reported N^6-(hydroxyacetyl)-2′-deoxyadenosine adduct. In the reaction of glyoxal with 2′-deoxycytidine and cytidine at neutral conditions and 37 °C, 5-hydroxyacetyl pyrimidine derivatives were obtained. When the cytidine reaction was performed at pH 4.5 and 50 °C, the 5-hydroxyacetyl derivative of uridine was formed through deamination of cytidine−glyoxal. Adducts in the thymidine reaction could not be detected. In the reaction of glyoxal with calf thymus DNA, the 2′-deoxyguanosine−glyoxal and 2′-deoxyadenosine−glyoxal adducts were obtained, the former being the major adduct.

Introduction

Glyoxal (ethanedial, Scheme 1) is an increasingly used industrial chemical with an annual worldwide production volume of about 120−170 kilotonnes (*1*). Glyoxal has a wide industrial use, and is for example used as a chemical intermediate in the production of pharmaceuticals and dyestuffs (*1*, *2*). It is also industrially employed as a cross-linking agent in the production of a large range of different polymers, such as textiles (e.g. permanent press fabrics), paper and proteins (*2*, *3*), as well as soil stabilizer and grouting systems, adding compressive strength to cement (*4*). In addition, glyoxal is used as a biocide and as an active ingredient in disinfectant products, often in preparation with other components such as formaldehyde, glutaraldehyde and quaternary ammonium compounds (*1*, *3*), for example as deodorizing agent in the crude oil and gas industry (H_2S scavenger) or in embalming fluids (*3*). Furthermore, glyoxal is also used as an insolubilizing agent for compounds containing polyhydroxyl groups (such as poly(vinyl alcohol), starch and cellulose materials) (*3*). Consequently, occupational exposure to glyoxal may occur in a number of industries.

Scheme 1

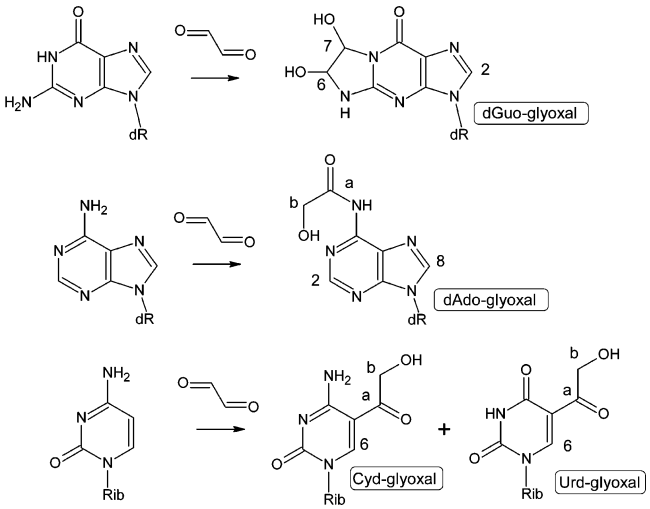

Glyoxal is endogenously produced during normal cellular metabolism by a multitude of enzyme independent pathways, such as the spontaneous reaction of amino groups in proteins with reducing sugars (Maillard reaction), sugar autoxidation, DNA oxidation, peroxidation

* To whom correspondence should be addressed. Tel: 358-2-215 4138. Fax: 358-2-215 4866. E-mail: leif.kronberg@abo.fi.
† National Institute of Occupational Health.
‡ Department of Chemistry, University of Oslo.
§ Department of Biology, University of Oslo.
⊥ Department of Organic Chemistry, Åbo Akademi University.

10.1021/tx0496688 CCC: $30.25
Published on Web 00/00/0000 PAGE EST: 9.1

of polyunsaturated fatty acids, and UV photodamage, and in conditions of oxidative stress and depletion of glutathione (*5*−*19*). In addition, glyoxal is a product of microsomal oxidation of compounds such as glycolaldehyde, ethylene glycol, and β-hydroxy-substituted N-nitrosamines and possibly contributes to the toxic, genotoxic, and tumorgenic action of these substances (*20*, *21*).

Glyoxal has been reported to be a potent allergen, and cross-sensizitation has been shown between glyoxal, formaldehyde and glutaraldehyde (*3*). Furthermore, the DNA damaging activity of glyoxal in rat liver and stomach is documented (*22*), while its tumor promoting activity in rat *N*-methyl-*N*′-nitro-*N*-nitrosoguanidine carcinogenesis has also been reported (*23*). Glyoxal induces point mutations, mainly at G:C-sites,[1] as well as deletions and frameshift mutations in bacteria and mammalian cells (*24*−*26*). To the authors knowledge, no studies with long-term exposure to glyoxal by inhalation or oral routes are available (*1*). Thus, data on carcinogenic effects to mammals are lacking.

Already four decades ago it was shown that glyoxal formed adducts with guanosine, adenosine and cytidine (*27*−*30*), where the adenosine and cytidine adducts were studied by means of UV spectra, while the structure of the guanosine adduct was elucidated by UV, IR and ^{1}H NMR spectra. The guanosine−glyoxal adduct was reported to be relatively stable, while the adenosine−glyoxal and cytidine−glyoxal adducts were found to be more labile (*30*). In 1998, Kasai et al. reacted glyoxal with DNA at physiological conditions, and elucidated the structure of the 2′-deoxycytidine−glyoxal adduct (5-hydroxyacetyl-2′-deoxycytidine) by UV, MS and ^{1}H and ^{13}C NMR spectra, and showed, as opposed to the earlier report, that glyoxal does not react at the exocyclic amino group but rather at position 5 on the ring (*31*). They also reported that the 2′-deoxyguanosine−glyoxal adduct is considerably more stable within the DNA structure, as compared to the nucleoside monomer. In addition, they demonstrated the formation of the bis-nucleosides 2′-deoxyguanosine−glyoxal−2′-deoxyguanosine, 2′-deoxycytidine−glyoxal−2′-deoxyguanosine and 2′-deoxyadenosine−glyoxal−2′-deoxyguanosine by the action of glyoxal on nucleosides and DNA (*31*). Due to low reaction yields at physiological conditions, the characterization of the bis-nucleosides was limited to UV and MS analyses. Furthermore, they detected 2′-deoxycytidine−glyoxal−2′-deoxyguanosine and 2′-deoxyadenosine−glyoxal−2′-deoxyguanosine in enzymatic hydrolysates of single stranded DNA treated with a high concentration of glyoxal (40:1), while a corresponding reaction with double stranded DNA was not reported. More recently, Brock et al. improved the reaction efficiency of the bis-nucleoside synthesis at nonphysiological conditions and elucidated the structures of 2′-deoxyguanosine−glyoxal−2′-deoxyguanosine, 2′-deoxycytidine−glyoxal−2′-deoxyguanosine, and 2′-deoxyadenosine−glyoxal−2′-deoxyguanosine by means of ^{1}H and ^{13}C NMR (*32*).

In this study we have reacted glyoxal with the deoxynucleosides and with cytidine in aqueous solutions. The formed adducts have been isolated and purified, and subjected to mass spectrometric and ^{1}H and ^{13}C NMR spectroscopic studies in order to determine their structures. We have characterized two previously unknown glyoxal adducts, a 2′-deoxyadenosine−glyoxal adduct and a uridine−glyoxal adduct. Furthermore, the previously identified cytidine−glyoxal adduct has now been fully characterized by ^{1}H and ^{13}C NMR analyses. In hydrolysate of calf thymus DNA, after glyoxal reaction with DNA, we detected small amounts of the 2′-deoxyadenosine−glyoxal adduct as well as the major adduct 2′-deoxyguanosine−glyoxal.

Experimental Section

Caution: *Glyoxal has been found to be mutagenic in bacteria and mammalian cells. Caution should therefore be exercised in the handling of the compound.*

Chemicals. Calf thymus DNA (Type I: sodium salt, highly polymerized), 2′-deoxyguanosine, 2′-deoxycytidine, 2′-deoxyadenosine, thymidine, cytidine, acid phosphatase (wheat germ Type I), alkaline phosphatase (E. coli Type III), nuclease P1 from Penicillum citrinum, bis-tris buffer (bis[2-hydroxyethyl]iminotris[hydroxymethyl]-methane hydrochloride),[1] and Me_2SO-d_6 were obtained from Sigma-Aldrich (St. Louis, MO). Glyoxal trimer dihydrate, 2′-deoxyuridine, and uridine were purchased from Fluka (Buchs, Switzerland). HPLC grade acetonitrile (ACN) and methanol (MeOH) were obtained from Rathburn Chemicals (Walkerburn, UK).[1] 96% ethanol (EtOH) was purchased from Arcus (Oslo, Norway).[1] Water was obtained from an Elgastat Maxima HPLC water purification system (Elga Ltd., Buckinghamshire, UK). Analytical grade ammonium acetate (NH_4Ac), zinc chloride ($ZnCl_2$), and magnesium chloride hexahydrate ($MgCl_2 \times 6H_2O$) were provided by Merck (Darmstadt, Germany).[1] Nitrogen, used as nebulizer and desolvation gas in the mass spectrometer, was produced by a Whatman nitrogen generator (Whatman International, Haverhill, MA).

Chromatographic System. LC analyses were performed on a Waters CapLC System (Waters, Milford, MA) consisting of a binary capillary gradient pump, an autosampler, and a diode array detector (DAD).[1] The DAD was operated in the 200 to 400 nm wavelength range. The reaction mixtures were chromatographed on a (3.5 μm, 1.0 mm i.d. $\times$ 150 mm) Kromasil C_{18} analytical column (G&T Septech, Kolbotn, Norway). The analytical chromatographic system was operated at ambient temperatures. The LC system was operated isocratically for 3 min with ACN and 10 mM NH_4Ac (2:98, v/v), prior to a gradient from 2% to 50% ACN over the course of 12 min at a flow rate of 40 μL/min. Semipreparative isolation of the products was performed on a (5 μm, 10 mm i.d. $\times$ 250 mm) Thermo Hypersil-Keystone BDS Hypersil C_{18} column (Thermo Electron Corporation, Waltham, MA). A (3.5 μm, 3.9 mm i.d. x 20 mm) Waters XTerra RP18 guard column was coupled to the semipreparative column. The semipreparative column was coupled to a Waters 600 multisolvent delivery system, a Waters 712 WISP autosampler, a Waters column heater module, and a Waters 490 UV detector. The semipreparative chromatographic system was operated at 30 °C and at flow rates ranging from 2.0 to 2.5 mL/min.

Spectroscopic and Spectrometric Methods. The NMR spectra were recorded at 30 °C on a Bruker Avance 600 NMR spectrometer (Bruker, Rheinstetten, Germany). The instrument was operated at field strengths of 600 and 150 MHz for recording the ^{1}H NMR and the ^{13}C NMR spectra, respectively. The carbon spectrum of the 2′-deoxyadenosine−glyoxal adduct was recorded on a JEOL JNM-A500 FT-NMR spectrometer (JEOL, Tokyo, Japan) which was operated at field strengths of 500 MHz. The NMR samples were dissolved in dry Me_2SO-d_6. The ^{1}H NMR signal assignments were based on chemical shifts and H−H and C−H correlation data. The assignment of carbon signals was based on chemical shifts, ^{13}C-^{1}H direct connectivities (HMQC) and ^{13}C-^{1}H long-range connectivities (HMBC).

[1] Abbreviations: G:C-sites, guanosine:cytidine-sites; Bis-tris, bis-[2-hydroxyethyl]iminotris[hydroxymethyl]-methane hydrochloride; ACN, acetonitrile; MeOH, methanol; EtOH, ethanol; NH_4Ac, ammonium acetate; $ZnCl_2$, zinc chloride; $MgCl_2 \times 6H_2O$, magnesium chloride hexahydrate; DAD, diode array detector; ESI, electrospray ionization; MRM, multiple reaction monitoring; RF, radio frequency; TOF, time-of-flight; HMBC, heteronuclear multiple bond connectivity NMR spectroscopy (long-range ^{1}H-^{13}C COSY).

Table 1. Mass Spectrometric Data of Nucleoside Adducts

nucleoside adduct	fragment				
	$[M+H]^+$	$[M+H-dR+H]^+$ [a]	$[2M+H]^+$	$[M+H-glyoxal]^+$	$[B+H]^+$ [b]
2′-deoxyguanosine−glyoxal	326	210	651	268	152
2′-deoxyadenosine−glyoxal	310	194		252	136
2′-deoxycytidine−glyoxal	286	170		228	112
cytidine−glyoxal	302	170	603	244	112
uridine−glyoxal	303	171		245	113

[a] dR is the deoxyribosyl or ribosyl moiety. [b] B is the corresponding base of the nucleoside.

The MS analyses of the column effluent were provided by a tandem quadrupole MS equipped with a Z-spray atmospheric pressure ionization source prepared for electrospray ionization (ESI) from Micromass (Manchester, UK).[1] ESI was performed in positive mode and the applied voltages were: capillary voltage: 4000 V; sample cone voltage: 15 V; and extraction cone voltage: 2 V. The nebulizer gas flow was 90 L/hour, the desolvation gas flow was 360 L/hour, the desolvation temperature was 450 °C and the source temperature was 110 °C. When the instrument was operated in the multiple reaction monitoring (MRM) mode, argon (99.999%) (Yara, Oslo, Norway) was used as collision gas, collision cell pressure was set to 2.8×10^{-3} mbar, and collision and RF lens voltages were set to 15 and 0.4 V,[1] respectively. The CapLC system and the tandem quadrupole MS instrument were controlled and data were acquired using MassLynx v3.5 software, and mass spectra were acquired in the 100−800 *m/z* range.

Exact mass determination was performed by direct infusion of the nucleoside adducts on a Micromass time-of-flight (TOF) MS equipped with a Z-spray atmospheric pressure ionization source prepared for ESI.[1] The TOF MS was operated at a resolution of 6200.

Small-Scale Reactions of Glyoxal with Nucleosides. Glyoxal (168 mg, 2.4 mmol) was reacted separately with 2′-deoxyguanosine (15 mg, 0.056 mmol), 2′-deoxyadenosine (15 mg, 0.060 mmol), 2′-deoxycytidine (15 mg, 0.066 mmol), cytidine (15 mg, 0.062 mmol), uridine (15 mg, 0.061 mmol), and thymidine (15 mg, 0.062 mmol), respectively, in 8 mL of 0.5 M phosphate buffer solutions at pH 4.5 and pH 7.4. The reactions were performed at 37 °C and 50 °C and were allowed to proceed for 7 days. The progress of the reactions was followed by LC-ESI tandem quadrupole MS analysis of aliquots of the reaction mixtures.

General Procedure for Preparative-Scale Reactions of Glyoxal with 2′-Deoxynucleosides and Nucleosides. To a solution of the deoxynucleoside or the nucleoside in 0.5 M phosphate buffer solutions (pH 4.5 or pH 7.4) glyoxal trimer dihydrate dissolved in 0.5 M phosphate buffer (pH 4.5 or pH 7.4) in order to obtain a 40 times excess of glyoxal was added. The reaction was stirred at 37 °C or 50 °C and monitored by LC-ESI tandem quadrupole MS measurements. At the conclusion of the reaction, the mixture was filtered and concentrated by rotary evaporation at 37 °C to about one-tenth of the initial volume. Precipitated phosphate buffer was removed by filtration. Separation and purification of adducts were carried out using the semipreparative instrumental setup at the conditions given below. The residues were analyzed as described below. The collected fractions containing the pure adduct were combined and rotary evaporated at 37 °C to dryness, further dried under vacuum overnight and finally dissolved in dry Me_2SO-d_6.

Preparation of the 2′-Deoxyguanosine-Glyoxal Adduct. The general procedure was used with 2′-deoxyguanosine (50 mg, 0.2 mmol), 0.5 M phosphate buffer (pH 7.4, 30 mL), and glyoxal trimer dihydrate (0.522 g, 2.5 mmol) with a reaction time of 2 h at 37 °C, essentially according to a procedure described by Kasai et al. (*31*). The adduct was purified on the semipreparative LC system which was operated isocratically for 6 min with ACN and 10 mM NH_4Ac (2:98, v/v), prior to a gradient from 2% to 10% ACN over the course of 8 min, and finally maintained at 10% ACN for 14 min at a flow rate of 2.5 mL/min. The collected fractions containing the adduct were combined and rotary evaporated at 37 °C to about one-tenth of the initial volume. Finally, the sample was desalted by using the semipreparative LC system, which was operated isocratically with MeOH and water (7:93, v/v) at a flow rate of 2.0 mL/min and the adduct fractions were collected and subjected to the general procedure described above.

The isolated adduct had the following spectral characteristics: 2′-deoxyguanosine−glyoxal, UV spectrum, UV_{max} 249 and 275 nm, and UV_{min} 223 nm. In the positive ion electrospray mass spectrum the following ions were observed (*m/z*, relative intensity, formation) (Table 1): 326, 100%, $[M+H]^+$; 210, 26%, $[M-C_5H_8O_3+H]^+$; 651, 8%, $[2M+H]^+$. High-resolution MS $C_{12}H_{15}N_5O_6$ calcd, 326.110; found, 326.116. The ^1H and ^{13}C NMR data are presented in Table 2.

Preparation of the 2′-Deoxyadenosine−Glyoxal Adduct. The general procedure was used with 2′-deoxyadenosine (2.0 g, 8 mmol), 0.5 M phosphate buffer (pH 4.5, 400 mL), and glyoxal trimer dihydrate (22.3 g, 106.1 mmol) with a reaction time of 4 days at 50 °C. The adduct was purified on the semipreparative LC system which was operated isocratically for 3 min with ACN and 10 mM NH_4Ac (2:98, v/v), prior to a gradient from 2% to 10% ACN over the course of 8 min, and finally maintained at 10% ACN for 7 min at a flow rate of 2.5 mL/min. Further purification of the adduct, after rotary evaporation at 37 °C to about one-tenth of the initial volume, was performed using a MeOH − 10 mM NH_4Ac gradient from 2% (5 min hold time) to 10% MeOH over the course of 10 min (maintained at 10% MeOH for 13 min) at a flow rate of 2.0 mL/min. The collected fractions containing the adduct were combined and rotary evaporated at 37 °C to about one-tenth of the initial volume. Finally, the sample was desalted by using the semipreparative LC system, which was operated isocratically with MeOH and water (7:93, v/v) at a flow rate of 2.0 mL/min and the adduct fractions were collected and subjected to the general procedure described above.

The isolated adduct had the following spectral characteristics: 2′-deoxyadenosine−glyoxal, UV spectrum, UV_{max} 213 and 267 nm, and UV_{min} 232 nm. In the positive ion electrospray mass spectrum the following ions were observed (*m/z*, relative intensity, formation) (Table 1): 310, 100%, $[M+H]^+$and 194, 7%, $[M-C_5H_8O_3+H]^+$. High-resolution MS $C_{12}H_{15}N_5O_5$ calcd, 310.115; found, 310.111. The ^1H and ^{13}C NMR data are presented in Table 3.

Preparation of the Cytidine−Glyoxal Adduct. When 2′-deoxycytidine was reacted with glyoxal, an adduct was obtained which underwent deglycolysation during purification and isolation. Therefore, the work on the structural characterization was performed on the adduct produced from the glyoxal and cytidine reaction.

The general procedure was used with cytidine (1.0 g, 4.1 mmol), 0.5 M phosphate buffer (pH 4.5, 200 mL), and glyoxal trimer dihydrate (11.52 g, 54.8 mmol) with a reaction time of 4 days at 50 °C. The adducts were purified on the semipreparative LC system which was operated isocratically for 3 min with ACN and 10 mM NH_4Ac (2:98, v/v), prior to a gradient from 2% to 15% ACN over the course of 13 min, and finally maintained at 15% ACN for 3 min at a flow rate of 2.5 mL/min. Further purification of the collected adducts, after rotary evaporated at 37 °C to about one-tenth of the initial volume, was performed on the semipreparative LC system with the same gradient. The collected fractions containing the adduct were combined and

Table 2. ^{1}H and ^{13}C Chemical Shifts (δ), Spin−Spin Coupling Constants, $J_{H,H}$ (Hz), of Protons, and Long-Range C−H Correlations (HMBC)[10] in the 2′-Deoxyguanosine−Glyoxal Adduct

proton	δ (ppm)	multiplicity	$J_{H,H}$ (Hz)	carbon	δ (ppm)	HMBC
H-2 (1H)	7.968	s		C-2[a]	135.74; 135.71	H-1′
				C-3a	150.68	H-1′; H-2
				C-9a[a]	117.64; 117.60	H-2
				C-4a[a]	154.73; 154.70	N*H*; H-2; H-6; H-7
				C-9	154.97	H-2
N*H* (1H)	8.815	s, br				
O*H*-7 (1H)[a,b]	7.243; 7.242	d	6.6			
O*H*-6 (1H)[a,b]	6.482; 6.481	d	7.4			
H-7 (1H)[b]	5.478	dd	6.5; 3.9	C-7[a]	84.20; 84.18	N*H*; H-6
H-6 (1H)[a,b]	4.871; 4.869	dd	7.4; 3.9	C-6[a]	83.78; 83.76	O*H*-7; O*H*-6; H-7
H-1′ (1H)[a]	6.127; 6.125	dd	7.5; 6.1	C-1′[a]	82.98; 82.96	H-2′
H-2′ (1H)[a]	2.222; 2.216	ddd	13.2; 6.1; 3.1	C-2′	39.68	H-3′
H-2″ (1H)	2.520	ddd	13.2; 7.6; 5.8			
H-3′ (1H)	4.341	qd	5.8; 3.1	C-3′	70.74	H-1′; O*H*-3′; H-4′; H-5′; H-5″
H-4′ (1H)[a]	3.825; 3.821	dt	∼3; ∼4.8	C-4′	87.72	H-2′; H-2″; O*H*-3′; H-3′; H-5′; H-5″
H-5′ (1H)[a]	3.564; 3.562	dt	11.8; 5.3	C-5′	61.70	O*H*-5′
H-5″ (1H)	3.501	ddd	11.8; 5.3; 4.8			
OH-3′ (1H)[a]	5.307; 5.302	d	4.1			
OH-5′ (1H)[a]	4.962; 4.958	t	5.5			

[a] Separate shifts due to the presence of a mix of diastereomers. [b] The coupling of 6.6 and 7.4 Hz disappeared upon addition of D_2O to the NMR sample.

Table 3. ^{1}H and ^{13}C Chemical Shifts (δ), Spin−Spin Coupling Constants, $J_{H,H}$ (Hz), of Protons, and Long-Range C−H Correlations (HMBC) in the 2′-Deoxyadenosine−Glyoxal Adduct

proton	δ (ppm)	multiplicity	$J_{H,H}$ (Hz)	carbon[a]	δ (ppm)	HMBC
H-8 (1H)	8.35	s		C-8	139.5	H-1′
H-2 (1H)	8.21	s		C-2	152.4	
				C-4	148.0	H-1′; H-8
				C-5	119.6	H-8
				C-6	153.9	H-2
N*H* (1H)	7.55	s, br				
O*H* (1H)	7.07	s, br				
H−b (2H)	3.95	s, br		C-b	44.3	
				C-a	172.0	H-b (weak)
H-1′ (1H)	6.35	dd	6.4; 7.4	C-1′	84.0	H-2′; H-3′
H-2′ (1H)	2.73	ddd	13.1; 7.6; 5.5	C-2′	39.5	
H-2″ (1H)	2.27	ddd	13.1; 6.1; 2.8			
H-3′ (1H)	4.42	dt	5.5; 2.7	C-3′	70.9	H-1′; H-2′; H-2″; H-5′; H-5″
H-4′ (1H)	3.88	dt	4.3; 2.4	C-4′	88.1	H-2′; H-2″; H-5′; H-5″
H-5′ (1H)	3.62	dd	11.9; 4.3	C-5′	61.9	
H-5″ (1H)	3.53	dd	11.9; 4.3			

[a] Spectrum recorded on the JEOL JNM-A500 instrument at 125 MHz.

rotary evaporated at 37 °C to about one-tenth of the initial volume. Finally, the sample was desalted by using the semi-preparative LC system, which was operated isocratically with MeOH and water (5:95, v/v) at a flow rate of 2.0 mL/min and the adduct fractions were collected and subjected to the general procedure described above.

The isolated adducts had the following spectral characteristics: Cytidine−glyoxal, UV spectrum, UV_{max} 222 and 287 nm, and UV_{min} 263 nm. In the positive ion electrospray mass spectrum the following ions were observed (*m/z*, relative intensity, formation) (Table 1): 302, 100%, $[M+H]^+$; 170, 24%, $[M-C_5H_8O_3+H]^+$; 603, 12%, $[2M+H]^+$. High-resolution MS $C_{11}H_{15}N_3O_7$ calcd, 302.099; found, 302.105. The ^{1}H and ^{13}C NMR data are presented in Table 4.

Uridine−glyoxal, UV spectrum, UV_{max} 227 and 286 nm, and UV_{min} 249 nm. In the positive ion electrospray mass spectrum the following ions were observed (*m/z*, relative intensity, formation) (Table 1): 303, 100%, $[M+H]^+$; 171, 61%, $[M-C_5H_8O_3+H]^+$. High-resolution MS $C_{12}H_{14}N_2O_8$ calcd, 303.083; found, 303.082. The ^{1}H and ^{13}C NMR data are presented in Table 5.

Molar Absorptivities. The NMR samples were after NMR analysis evaporated to dryness under vacuum for 24 h and 0.02 mg/mL solutions were prepared in EtOH and water (80:20, v/v). The molar absorptivities (ϵ) of the 2′-deoxyguanosine−glyoxal (249 nm), 2′-deoxyadenosine−glyoxal (267 nm), cytidine−glyoxal (287 nm) and uridine−glyoxal (286 nm) adducts were measured to 8300, 9300, 7800, and 6300, respectively, using a Shimadzu (Kyoto, Japan) MPS-2000 double beam spectrophotometer.

Determination of Nucleoside Adduct Yields. The quantitative determinations of adducts in the reaction mixtures were made using the calibration curve obtained from standard solutions made from the dried NMR samples. The adducts were quantified using LC-ESI tandem quadrupole MS in MRM mode. The molar yields were calculated from the original amount of nucleoside in the reaction mixture.

Reactions of Glyoxal with Calf Thymus DNA. Glyoxal (17.5 mg, 0.25 mmol) was reacted with double-stranded calf thymus DNA (2.5 mg) in 2.5 mL of 0.1 M phosphate buffer (pH 7.4) at 37 °C. The mixture was stirred for 48 h and then transferred to a 50 mL NUNC (Nalge Nunc Int., Rochester, NY) centrifuge tube. The DNA was precipitated by addition of 5 M NaCl (0.5 mL), cold EtOH (8 mL), and the solution was cooled at −20 °C. The mixture was centrifuged (10 min at 3000 rpm), and the supernatant was removed. The recovered DNA was washed with cold 70% EtOH (3 mL), cold EtOH (3 mL), and dissolved in water (3 mL). The DNA was reprecipitated from the solution by addition of cold EtOH (8 mL), cooled to −20 °C, and recovered by centrifuging. The DNA was dried in a vacuum

Table 4. ^{1}H and ^{13}C Chemical Shifts (δ), Spin−Spin Coupling Constants, $J_{H,H}$ (Hz), of Protons, and Long-Range C−H Correlations (HMBC) in the Cytidine−Glyoxal Adduct

proton	δ (ppm)	multiplicity	$J_{H,H}$ (Hz)	carbon	δ (ppm)	HMBC
N*H* (1H)[a]	7.99	d	3.7			
N*H* (1H)[a]	8.30	d	4			
H-6 (1H)	9.08	s		C-6	148.89	H-1′
H-b_1 (1H)	4.51	dd	17.4; 6.0	C-b	63.99	O*H*-9
H-b_2 (1H)	4.47	dd	17.4; 6.0			
O*H*-9 (1H)[a]	4.99	t	6.1			
				C-a	197.06	H-6; O*H*-b; H-b_1; H-b_2
				C-2	152.79	N*H*(8.3); H-1′
				C-4	163.02	H-6
				C-5	100.68	N*H*(8.0); H-6
H-1′ (1H)	5.73	d	1.9	C-1′	90.69	
H-2′ (1H)	3.97	dt	1.9; 4.6	C-2′	74.82	
H-3′ (1H)	4.02	dt	4.7; 7.0	C-3′	67.76	
H-4′ (1H)	3.92	dt	2.1; 7.6	C-4′	83.60	
H-5′ (1H)	3.82	ddd	12.2; 4.5; 2.5	C-5′	58.98	
H-5″ (1H)	3.64	ddd	12.2, 4.5; 1.9			
OH-2′ (1H)[a]	5.57	d	4.8			
OH-3′ (1H)[a]	5.03	d	6.6			
OH-5′ (1H)[a]	5.48	t	4.6			

[a] Signal lost when shaken with D_2O.

Table 5. ^{1}H and ^{13}C Chemical Shifts (δ), Spin−Spin Coupling Constants, $J_{H,H}$ (Hz), of Protons, and Long-Range C−H Correlations (HMBC) in the Uridine−Glyoxal Adduct

proton	δ (ppm)	multiplicity	$J_{H,H}$ (Hz)	carbon	δ (ppm)[a]	HMBC
H-6 (1H)	8.82	s		C-6	146.8	H-1′
H-b_1 (1H)	4.50	br		C-b	68.0	
H-b_2 (1H)	4.50	br				
				C-a	195.3	H-6; H-b_1,H-b_2
				C-2	150.0	H-6
				C-4	161.1	H-6
				C-5	*c*	
H-1′ (1H)	5.78	d	4.2	C-1′	89.0	
H-2′ (1H)	4.08	q	4.6	C-2′	74.3	
H-3′ (1H)	3.97	q	5.1	C-3′	69.6	
H-4′(1H)	3.91	m	*b*	C-4′	84.9	
H-5′(1H)	3.68	ddd	12.0; 4.5; 2.9	C-5′	60.2	
H-5″ (1H)	3.57	ddd	12.9; 4.3; 3.2			
OH-2′ (1H)	5.48	d	5.3			
OH-3′ (1H)	5.13	d	5.4			
OH-5′ (1H)	5.18	t	4.6			

[a] Chemical shift assigned through one bond C−H correlations. [b] Could not be determined due to overlapping from a signal of an impurity. [c] Signal not found in the C−H correlation spectrum.

for 5 h and then dissolved in 4 mL of 100 mM bis-tris buffer (pH 6.5) containing 2 mM $MgCl_2$ overnight. The DNA was enzymatically hydrolyzed as follows. To the DNA solution was added Nuclease P1 (dissolved in a concentration of 1 mg/mL in 1 mM $ZnCl_2$) to obtain a concentration of 50 units/mL. The mixture was incubated in a shaking water bath at 37 °C for 4 h. Finally, bacterial alkaline phosphatase and wheat germ acid phosphatase (the latter dissolved in bis-tris-$MgCl_2$ buffer at a concentration of 10 mg/mL) were added to give a final concentration of 6 units/mL and 0.4 units/mL, respectively. The mixture was incubated at 37 °C for 18 h. The enzyme digest mixture was loaded onto a prerinsed (water) Centricon YM-3 filter from Millipore (Billerica, MA) and centrifuged with a Sorvall (Kendro Laboratory Products, Asheville, NC) Superspeed fixed angle rotor (SS-34) for 150 min (10 °C) at 7000 rpm. The ultrafiltrate was recovered and concentrated with rotary evaporation at 37 °C to near dryness and reconstituted in 600 μL water. The resulting solution was analyzed with LC-ESI tandem quadrupole MS.

Quantification of DNA Adducts and 2′-Deoxyuridine. The quantification of DNA adducts and 2′-deoxyuridine in the DNA hydrolysate was made by LC-ESI tandem quadrupole MS in MRM mode. The adducts obtained from the DNA hydrolysate were quantified with the calibration curve obtained from standard solutions made from the dried NMR samples. The 2′-deoxyuridine obtained from the DNA hydrolysate was quantified with the calibration curve obtained from standard solutions.

Results and Discussion

Reactions of Glyoxal with Nucleosides. The small-scale reactions of glyoxal with each of the four deoxyribose nucleosides and with the ribose nucleoside cytidine were performed at various conditions. The conditions giving the highest yields of the adducts were applied in large-scale reactions from which the adducts were subsequently isolated. The reactions were monitored by analytical LC with both DAD and ESI tandem quadrupole MS detection and examples of the chromatographic profiles for the reaction mixtures are shown in Figures 1 and 2.

From larger-scale reactions, the adducts were isolated by semipreparative LC and characterized by UV, NMR and MS analyses.

In the glyoxal reaction with 2′-deoxyguanosine, one adduct was formed (Figure 1A). The highest yield (99.8%) of the adduct was obtained after 2 h at neutral conditions and 37 °C. On the basis of spectroscopic and spectrometric methods, the adduct was identified as the previously known 2′-deoxyguanosine−glyoxal adduct, 3-(2′-deoxy-β-D-erythro-pentofuranosyl)-5,6,7-trihydro-6,7-dihydroxyimidazo[1,2-a]purine-9-one (Scheme 1). The positive ion electrospray mass spectrum of the 2′-

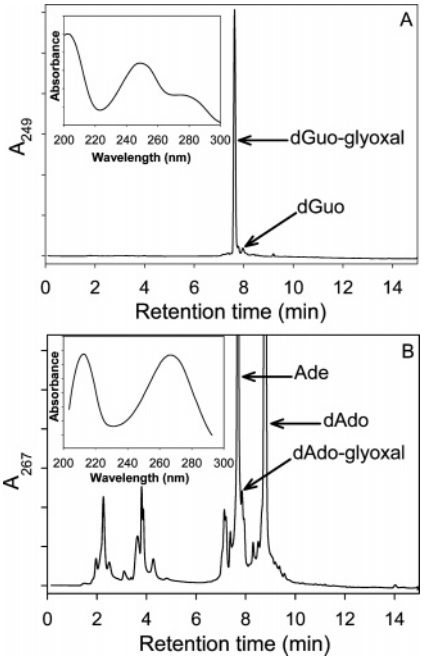

Figure 1. (A) C18 analytical column LC−UV chromatogram at 249 nm of the reaction mixture of glyoxal with 2′-deoxyguanosine in 0.5 M phosphate buffer (pH 7.4) held at 37 °C for 2 h and the UV spectrum of the 2′-deoxyguanosine−glyoxal adduct. (B) C18 analytical column LC−UV chromatogram at 267 nm of the reaction mixture of glyoxal with 2′-deoxyadenosine in 0.5 M phosphate buffer (pH 4.5) held at 50 °C for 4 days and the UV spectrum of the 2′-deoxyadenosine−glyoxal adduct.

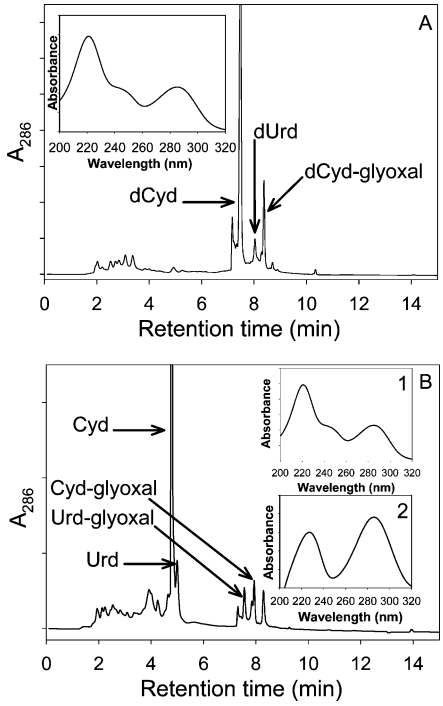

Figure 2. (A) C18 analytical column LC−UV chromatogram at 286 nm of the reaction mixture of glyoxal with 2′-deoxycytidine in 0.5 M phosphate buffer (pH 7.4) held at 37 °C for 4 days and the UV spectrum of the 2′-deoxycytidine−glyoxal adduct. (B) C18 analytical column LC−UV chromatogram at 286 nm of the reaction mixture of glyoxal with cytidine in 0.5 M phosphate buffer (pH 4.5) held at 50 °C for 4 days and the UV spectra of the (1) cytidine−glyoxal adduct and the (2) uridine−glyoxal adduct.

deoxyguanosine−glyoxal adduct (Table 1) showed a protonated molecular ion at *m/z* 326 and a fragment at *m/z* 210, which resulted from the cleavage of the deoxyribosyl moiety from the protonated molecular ion. In addition, the product ion scan of *m/z* 210 showed a fragment at *m/z* 152 corresponding to guanine. The ^{1}H NMR data recorded were almost identical to those reported by Brock et al. (*32*). Along with the ^{1}H NMR, the ^{13}C NMR data are presented in Table 2 and as far as we know, carbon chemical shifts for the compound have not been reported previously. In the table, the assignment of H-6 and H-7 is in accordance with that of Brock et al. and is based on the COSY spectrum where a slightly stronger correlation can be seen from the 5-NH to the signal at $\delta = 4.87$ ppm than to the signal at $\delta = 5.48$ ppm. However, this is not a definitive proof for correct assignment of the signals. In the long-range C−H correlation spectrum, the carbon at $\delta = 84.20$, which is connected to the proton at $\delta = 5.48$ ppm, showed a correlation to NH, while this correlation was not observed from the carbon at $\delta = 83.78$ ppm. Since the five membered ring is displaced from planarity by about 10° (*33*), this correlation is probably to C-6 and not C-7 and consequently, the assignment of C-6 and C-7 and of H-6 and H-7 are the reverse to that given in Table 2. However, a definitive assignment of the signals remains to be done. In the ^{1}H NMR and ^{13}C NMR spectra, several proton and carbon signals were observed as two sets of signals. This shows that the adduct was obtained as a pair of diastereomers. The small coupling observed between H-6 and H-7 ($J = 3.9$ Hz) supports a trans arrangement of the hydrogens and fits the results of the ab initio calculations of Loeppky et al. (*33*) where the dihedral angle between H-6 and H-7 was found to be 119.7°.

Recently, Brock et al. (*32*) have shown that the 2′-deoxyguanosine−glyoxal adduct connected to another unit of 2′-deoxyguanosine. In our study, however, any conjugate formation between the 2′-deoxyguanosine−glyoxal adduct and 2′-deoxyguanosine could not be observed. This is likely due to almost complete consumption of 2′-deoxyguanosine in the presence of excess glyoxal and thus no free 2′-deoxyguanosine remains in solution for reaction with the 2′-deoxyguanosine−glyoxal adduct.

In the reaction of glyoxal with 2′-deoxyadenosine, the small peak on the tail of the larger peak marked adenine (Ade) was on the basis of LC-ESI tandem quadrupole MS analysis tentatively determined as a 2′-deoxyadenosine−glyoxal adduct (Figure 1B). The adduct was obtained at the highest yield (0.51%) after 4 days of reaction at pH 4.5 and 50 °C. About 3 times lower yield was obtained in a reaction carried out at neutral conditions and 37 °C. On the basis of the MS, NMR and UV data, the 2′-deoxyadenosine−glyoxal adduct was identified as N^6-(hydroxyacetyl)-2′-deoxyadenosine (Scheme 1). In the mass spectrum of the peak, the fragment at *m/z* = 194 corresponded to the loss of the deoxyribosyl moiety from the protonated molecular ion at *m/z* = 310. Furthermore, the product ion scan of *m/z* =194 showed a fragment at *m/z* = 136 corresponding to adenine. In comparison to the UV spectrum of 2′-deoxyadenosine, the spectrum of the adduct (Figure 1B) shows a small red shift similar to the spectral changes Broude et al. (*30*) observed in the reaction mixtures of adenosine and glyoxal and that observed for the N^6-(hydroxymethylene)-adenine adduct generated from formaldehyde (*34*−*36*). The ^{1}H NMR spectrum displayed, besides the signals from the protons of the deoxyribose unit, purine proton signals at $\delta = 8.346$

and 8.205 ppm, which were assigned to H-8 and H-2, respectively (Table 3). Moreover, the spectrum showed three broadened singlet signals at $\delta = 7.552$, 7.072, and 3.948 ppm. From the intensity of the signals it was noted that the signal at $\delta = 3.948$ ppm was a two proton signal, while the other signals were due to single protons. In the short-range C−H spectrum (HMQC), a correlation was observed between the signal at $\delta = 3.948$ ppm and the signal at $\delta = 44.3$ ppm. The other two signals did not show correlations to any carbon absorbances and were consequently due to an amino or a hydroxyl function. Furthermore, the H−H correlation spectrum showed a correlation between the signal at $\delta = 7.552$ ppm and $\delta = 3.948$ ppm. We assigned the latter signal to the methylene protons (H−b) in the hydroxyacetyl group and the former to the exocyclic amino proton of the purine unit (*37*). The carbonyl carbon gave resonance at $\delta = 172.0$ ppm and this signal showed a long-range C−H correlation to the methylene protons.

The reaction of glyoxal with 2′-deoxycytidine at neutral conditions resulted in the formation of a 2′-deoxycytidine adduct and in deamination of 2′-deoxycytidine yielding 2′-deoxyuridine (Figure 2A). The MS data gave a molecular weight of 285 for the adduct (Table 1). This indicated that the adduct contained a hydroxyacetyl unit. Isolation and purification of the adduct was found to cause deglycosidation and the pyrimidine adduct was obtained. Since the structural assignment by NMR, especially the site of adduction, could be simplified by working with a ribonucleoside adduct, we decided to perform the glyoxal reactions with the more stable ribose derivative of cytosine. It was found that when glyoxal was reacted with cytidine at pH 4.5 and 50 °C, a stable cytidine−glyoxal adduct was formed. The highest yield (0.35%) was noted after 3 days of reaction (Figure 2B).

On the basis of spectroscopic and spectrometric methods, the cytidine−glyoxal adduct was identified as 5-hydroxyacetyl-cytidine (Scheme 1). The positive ion mass spectrum of the cytidine−glyoxal adduct (Table 1) showed a protonated molecular ion at $m/z = 302$, which is 16 mass units higher than the corresponding 2′-deoxycytidine adduct and is the mass that should be obtained from an adduct consisting of a hydroxyacetyl moiety and cytidine. The fragment at $m/z = 170$ resulted from the cleavage of the ribosyl moiety from the protonated molecular ion. Furthermore, the product ion scan of m/z 170 showed a fragment at m/z 112 corresponding to cytosine.

In the ^{1}H NMR spectrum, the only observable proton signal that originates from the pyrimidine ring was the H-6 proton signal at $\delta = 9.077$ ppm (Table 4). The lack of resonance from the H-5 pyrimidine proton shows that the adduction has taken place at C-5 in the ring. The large downfield shift of H-6 can be explained by conjugation to the electronegative carbonyl group, C−a. The amount of water in the NMR sample was lower than that in the 2′-deoxyadenosine−glyoxal sample and therefore the exchangeable protons produced sharper resonance signals. The hydroxyl proton of the hydroxyacetyl group appeared as a triplet and the nonequivalent methylene protons (H−b_1, H−b_2) were observed as doublets of doublets. The C−b signal was observed at $\delta = 63.99$ ppm and the signal showed C−H long-range correlation to the hydroxyl function. The carbonyl carbon, C−a, gave a resonance signal at $\delta = 197.06$ ppm and the signal showed long-range correlations to H-6, the hydroxyl

Scheme 2

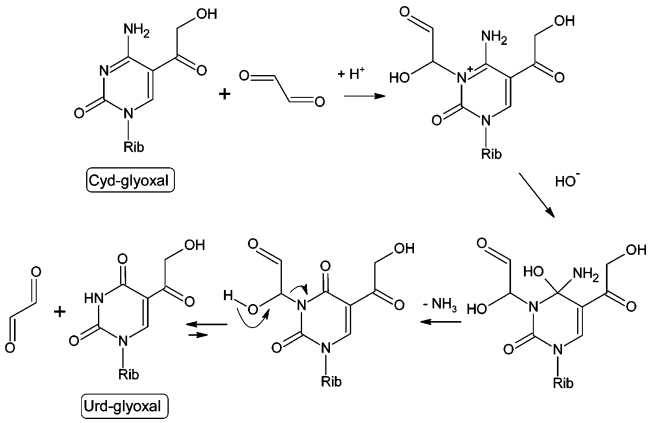

Scheme 3

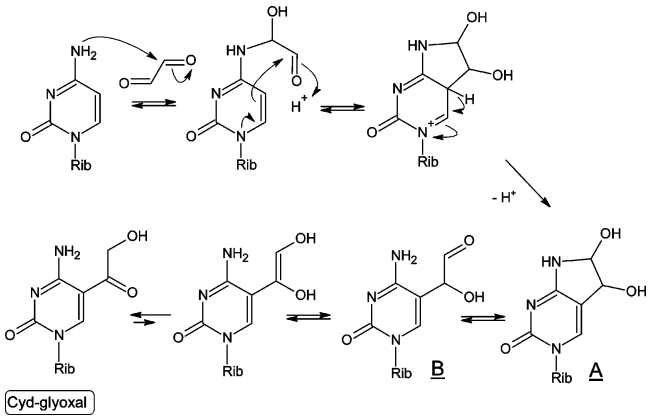

group and the H−b protons. The protons of the exocyclic amino group were not chemically equivalent and showed resonance signals at $\delta = 7.993$ and 8.300 ppm. This may be due to formation of an intramolecular hydrogen bond between one of the amino protons and the carbonyl oxygen in the hydroxyacetyl group.

In the reaction mixture of cytidine and glyoxal, a product peak with a mass one unit higher than the cytidine−glyoxal adduct was observed. This peak reached maximum intensity after 4 days of reaction and was found to be due to a uridine−glyoxal adduct (yield 1.53%). On the basis of the MS, NMR and UV data, the uridine−glyoxal adduct was identified as 5-hydroxyacetyl-uridine (Scheme 1). The UV spectrum of the uridine−glyoxal adduct is shown in Figure 2B. The positive ion electrospray mass spectrum of the uridine−glyoxal adduct (Table 1) showed a protonated molecular ion at m/z 303. The fragment at m/z 171 resulted from the cleavage of the ribosyl moiety from the protonated molecular ion. In addition, the product ion scan of m/z 171 showed a fragment at m/z 113 corresponding to uracil. The fragmentation pattern is equal to that of the cytidine−glyoxal adduct, but the masses of the fragments are one unit higher than that of the cytidine−glyoxal adduct. This indicates that the pyrimidine base unit of the adduct is uracil instead of cytosine.

Since the NMR sample contained low amounts of the compound, the carbon shifts could not be determined directly by ^{13}C NMR. Therefore the shifts were obtained from the C−H long-range correlation spectrum. In the ^{1}H NMR spectrum, the signal from the pyrimidine ring gave resonance at $\delta = 8.88$ ppm (Table 5). The signal

Table 6. Retention Times and Recorded Transitions of Nucleoside Adducts Analyzed in the DNA Hydrolysate

nucleoside adduct	retention time (min)	transition	mode of formation[a]	cone voltage (V)	collision energy (eV)
2′-deoxyguanosine−glyoxal	8.03	326 → 210	$MH^+ - dR + H$	15	15
2′-deoxyadenosine−glyoxal	8.73	310 → 194	$MH^+ - dR + H$	15	15
2′-deoxycytidine−glyoxal	*b*	286 → 170	$MH^+ - dR + H$	15	15
2′-deoxyuridine−glyoxal	*b*	287 → 171	$MH^+ - dR + H$	15	15

[a] dR is the deoxyribosyl moiety. [b] Not detected.

showed long-range C−H correlation to H′-1 of the ribose unit. The hydroxyl signals could not be observed due to the presence of water in the sample. Two separate signals at $\delta = 4.54$ were observed for the H−b protons. The carbon shift for the C−b atom was observed at $\delta = 68.0$ ppm, while the carbonyl carbon was observed at $\delta = 195.3$ ppm. The carbonyl carbon showed C−H long-range correlations to H-6 and the H−b protons.

It could be expected that the uridine−glyoxal adduct is obtained either by reaction of glyoxal with uridine or by deamination of the cytidine−glyoxal adduct. However, we found that uridine did not react with glyoxal and that the cytidine−glyoxal adduct did not undergo deamination at the conditions (pH 4.5 and 50 °C) where the uridine−glyoxal adduct was detected. On the other hand, the uridine−glyoxal adduct was formed in a solution of the cytidine−glyoxal adduct and glyoxal stored at pH 4.5 and 50 °C. This observation may be explained by attack of glyoxal on N-3 of the cytidine−glyoxal adduct yielding a cation which undergoes the deamination (Scheme 2) and a uridine derivative is formed. Subsequently, the glyoxal unit bound at N-3 in the uridine derivative is split off and the uridine−glyoxal adduct is obtained.

As far as we know, the only carbonyl compound shown to react at C-5 of cytidine is glyoxal. The C-5 carbon is nucleophilic and could attach the electrophilic carbonyl carbon in glyoxal. However, several studies (*38*−*41*) have shown that the exocyclic amino group in cytidine reacts readily with aldehyde groups and this could be the initial reaction in this case also (Scheme 3). The product, a carbinolamine, is unstable, and the starting material may be obtained. But, the carbinolamine could also undergo an intramolecular reaction where the second carbonyl group of glyoxal is attacked by the C-5 pyrimidine carbon and the cyclic intermediate *A* is formed. Finally, *A* will undergo ring-opening and *B* is formed which yields the cytidine−glyoxal adduct through keto−enol tautomerism.

In the chromatograms of reaction mixtures of glyoxal and 2′-deoxycytidine, and cytidine a peak corresponding to 2′-deoxyuridine and to uridine could be observed (Figure 2). The uridine nucleosides were identified on the basis of retention time equability with standards and on the basis of UV and MS. The formation of 2′-deoxyuridine in the 2′-deoxycytidine reaction with glyoxal has been previously observed by Kasai et al. (*31*) They proposed a mechanism for the cytidine deamination involving a cyclic intermediate formed by attack of glyoxal on N-3 and the exocyclic amino group of cytidine. The intermediate was suggested to facilitate the hydrolytic deamination of cytidine.

No adducts were found in the reaction mixture of glyoxal and thymidine.

Reaction of Glyoxal with DNA. The reaction of glyoxal with double stranded calf thymus DNA was performed at pH 7.4 at 37 °C for 2 and 7 days, and the modified DNA was enzymatically hydrolyzed to deoxynucleosides. The adducts were identified by comparison

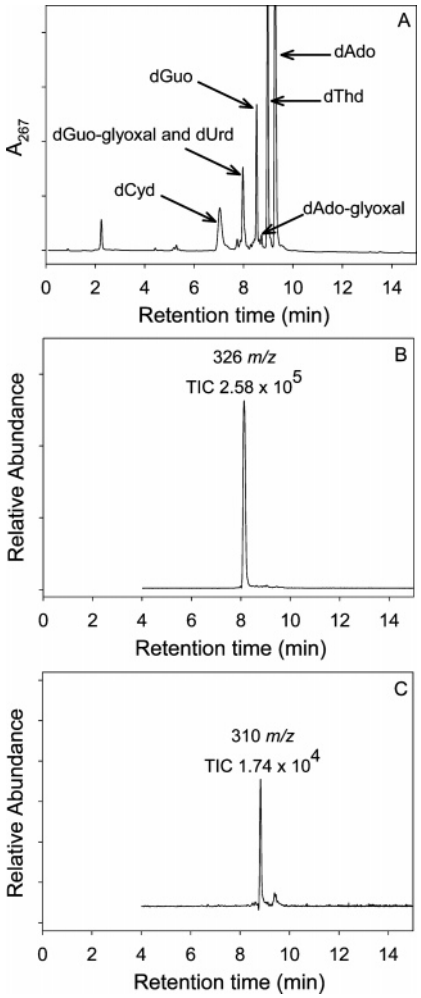

Figure 3. (A) C18 analytical column LC−UV chromatogram at 267 nm of the DNA hydrolysate of the 48 h dsDNA reaction with glyoxal, (B) MRM chromatogram of 2′-deoxyguanosine−glyoxal (326 *m/z* to 210 *m/z*), and (C) MRM chromatogram of 2′-deoxyadenosine−glyoxal (310 *m/z* to 194 *m/z*).

of their UV spectra, by the data obtained by LC-ESI tandem quadrupole MS in both scan and MRM (Table 6) modes and retention time equability with the deoxynucleoside standards. The major adduct was identified as the 2′-deoxyguanosine−glyoxal adduct (Figure 3). Following reaction times of 2 and 7 days the level of the adduct formed in DNA corresponded to 124 nmol/mg DNA (3800 adducts/10^5 nucleotides) and 147 nmol/mg DNA (4500 adducts/10^5 nucleotides), respectively. In addition, 2′-deoxyadenosine−glyoxal was detected in the DNA hydrolysate at levels of 0.202 nmol/mg DNA (62 adducts/10^5 nucleotides) and 0.201 nmol/mg DNA (46 adducts/10^5 nucleotides) following reaction times of 2 and 7 days, respectively. The corresponding level of 2′-deoxyuridine formed during the reactions was 67 nmol/mg DNA (2000 nucleosides/10^5 nucleotides) and 130 nmol/mg DNA (4000 nucleosides/10^5 nucleotides) at 2 and

7 days of reaction, respectively. The 2′-deoxycytidine−glyoxal and 2′-deoxyuridine−glyoxal adducts were not observed in the DNA hydrolysate.

Conclusions

Two previously unknown adducts formed in the reactions between glyoxal and nucleosides have been isolated and fully characterized by spectroscopic and spectrometric methods. The compounds were identified as 5-hydroxyacetyl-uridine and N^6-(hydroxyacetyl)-2′-deoxyadenosine adducts. Furthermore, the glyoxal adduct of cytidine was fully characterized and it was shown that the base modification was identical to that of the previously identified 5-hydroxyacetyl-2′-deoxycytidine adduct. In reaction of glyoxal with calf thymus DNA, small amounts of the N^6-(hydroxyacetyl)-2′-deoxyadenosine adduct was formed in addition to the 2′-deoxyguanosine−glyoxal adduct, which is the major DNA adduct. Also formed in DNA was 2′-deoxyuridine, which was probably derived from 2′-deoxycytidine by the deamination caused by the interaction of glyoxal.

The present work enhance the understanding of which adducts glyoxal can form in vitro, which is an important prerequisite to perform biological analysis both in cell culture and later in whole animals. It is well-known that the major adducts not always are the biological most important adduct (e.g. methylation). Glyoxal have yielded positive response in several genotoxic test systems. However, which adducts that are most mutagenic and possibly carcinogenic are not known.

Acknowledgment. Financial support from The Research Council of Norway is acknowledged.

References

(1) OECD (2002) OECD integrated HPV database, Paris, Organisation for economic cooperation and development, Available at http://cs3-hq.oecd.org/scripts/hpv.

(2) World Health Organisation (2004) *Glyoxal*, Concise International Chemical Assessment Document 57, pp 1−43

(3) Lundberg, P. (1995) The nordic expert group for criteria documentation of health risks from chemicals, Glyoxal, *Arbete och Hälsa 2*, 1−17.

(4) BASF (2003) Glyoxal product information, Available at http://www.basf.com/static/OpenMarket/Xcelerate/Preview_cid-974236975723_pubid-974236725646_c-Article.html.

(5) Loidl-Stahlhofen, A., Spiteller, G. (1994) α-Hydoxyaldehydes products of lipid peroxidation, *Biochim. Biophys. Acta 1211* (2), 156−160.

(6) Shibamoto, T. (1994) The role of lipid peroxidation caused by ultraviolet light in skin diseases, *J. Toxicol., Cutaneous Ocul. Toxicol. 13*, 193−202.

(7) Murata-Kamiya, N., Kamiya, H., Iwamoto, N., and Kasai, H. (1995) Formation of a mutagen, glyoxal, from DNA treated with oxygen free radicals, *Carcinogenesis 16*, 2251−2253.

(8) Murata-Kamiya, N., Kamiya, H., Muraoka, M., Kaji, H., and Kasai, H. (1997) Comparisons of oxidation products from DNA components by gamma-irradiation and Fenton-type reactions, *J. Radiat. Res. 38*, 121−131.

(9) Wells-Knecht, K. J., Zyzak, D. V., Lichtfield, J. E., Thorpe, S. R., and Baynes, J. W. (1995) Mechanism of autoxidative glycosylation: identification of glyoxal and arabinose as intermediates in the autoxidative modification of proteins by glucose, *Biochemistry 34*, 3702−3709.

(10) Fu, M.-X., Requena, J. R., Jenkins, A. J., Lyons, T. J., Baynes, J. W., and Thorpe, S. R. (1996) The advanced glycation end product, N^{ε}-(carboxymethyl)lysine, is a product of both lipid peroxidation and glycoxidation reactions, *J. Biol. Chem. 271*, 9982−9986.

(11) Mlakar, A., and Spiteller, G. (1996) Previosly unknown aldehydic lipid peroxidation compounds of arachidonic acid, *Chem. Phys. Lipids 79*, 47−53.

(12) Abardo, E. A., Minhas, H. S., and Thornalley, P. J. (1999) Accumulation of α-oxoaldehydes during oxidative stress: a role in cytotoxity, *Biochem. Pharmacol. 58*, 641−648.

(13) Miyata, T., and Kurokawa, K. (1999) Carbonyl stress: increased carbonyl modification of proteins by autoxidation products of carbohydrates and lipids in uremia, *Int. J. Artif. Organs 22*, 195−198.

(14) Thornalley, P. J., Langborg, A., and Minhas, H. S. (1999) Formation of glyoxal, methylglyoxal and 3-deoxyglucosone in the glycation of proteins by glucose, *Biochem. J. 344*, 109−116.

(15) Kasper, M., and Funk, R. H. W. (2001) Age-related changes in cells and tissues due to advanced glycation end products (AGEs), *Arch. Gerontol. Geriat. 32*, 233−243.

(16) Ulrich, P., and Cerami, A. (2001) Protein glycation, diabetes, and aging, *Recent Prog. Horm. Res. 56*, 1−24.

(17) Kasai, H. (2002) Chemistry-based studies on Oxidative DNA damage: formation, repair, and mutagenesis, *Free Radical Biol. Med. 33*, 450−456.

(18) Thornalley, P. J. (2002) Glycation in diabetic neuropathy: characteristics, consequences, causes, and therapeutic options, *Int. Rev. Neurobiol. 50*, 37−57.

(19) Wondrak, G. T., Cervantes-Laurean, D., Roberts, M. J., Qasem J. G., Kim, M., Jacobsen, E. L., and Jacobsen, M. K. (2002) Identification of α-dicarbonyl scavengers for cellular protection against carbonyl stress, *Biochem. Pharmacol. 63*, 361−373.

(20) Loeppky, R. N., and Goelzer, P. (2002) Microsome-mediated oxidation of *N*-nitrosodiethanolamine (NDELA), a bident carcinogen, *Chem. Res. Tocicol. 15*, 457−469.

(21) Loeppky, R. N., Ye, Q., Goelzer, P., and Chen Y. (2002) DNA adducts from *N*-nitrosodiethanolamine and related β-oxidized nitrosamines in vivo: 32P-postlabeling methods for glyoxal- and O6-hydroxyethyldeoxyguanosine adducts, *Chem. Res. Toxicol. 15*, 470−482.

(22) Furihata, C., Yoshida, S., and Matsushima, T. (1985) Potential initiating and promoting activities of diacetyl and glyoxal in rat stomach mucosa, *Jpn. J. Cancer Res. 76*, 809−814.

(23) Takahashi, M., Okamiya, H., Furukawa, F., Toyoda, K., Sato, H., Imaida, K., and Hayashi, Y. (1989) Effects of Glyoxal and methylglyoxal administration on gastric carcinogenesis in Wistar rats after initiation with *N*-methyl-*N*′-nitro-*N*-nitrosoguanidine, *Carcinogenesis 10*, 1925−1927.

(24) Murata-Kamiya, N., Kaji, H., and Kasai, H. (1997) Types of mutation induced by glyoxal, a major oxidative DNA damage product, in *Salmonella typhimurium*, *Mutat. Res. 37*, 13−16.

(25) Murata-Kamiya, N., Kamiya, H., Kaji, H., and Kasai, H. (1997) Mutational specificity of glyoxal, a product of DNA oxidation, in the lacI gene of wild type *Escherichia coli* W3110, *Mutat. Res. 377*, 255−262.

(26) Murata-Kamiya, N., Kamiya, H., Kaji, H., and Kasai, H. (1997) Glyoxal, a major product of DNA oxidation, induces mutation at G:C sites on a shuttle vector plasmid replicated in mammalian cells, *Nucleic Acids Res. 25*, 1897−1902.

(27) Staehelin, M. (1959) Inactivation of virus nucleic acid with glyoxal derivatives, *Biochim. Biophys. Acta 31*, 448−454.

(28) Shapiro, S., and Hachmann, J. (1966) The reaction of guanine derivatives with 1,2-dicarbonyl compounds, *Biochemistry 5*, 2799−2807.

(29) Shapiro, R., Cohen, B. I., Shiuey, S.-J., and Maurer, H. (1969) On the reaction of guanine with glyoxal, pyruvaldehyd, and kethoxal, and the structures of acylguanines. A new synthesis of N^2-alkylguanines, *Biochemistry 8*, 238−245.

(30) Broude, N. E., and Budowsky, E. I. (1971) The reaction of glyoxal with nucleic acid components III. Kinetics of the reaction with monomers, *Biochim. Biophys. Acta 254*, 380−388.

(31) Kasai, H., Iwamoto-Tanaka, N., and Fukada, S. (1998) DNA modifications by the mutagen glyoxal: adduction to G and C, deamination of C and GC and GA cross-linking, *Carcinogenesis 19*, 1459−1465.

(32) Brock, A. K., Kozelov, I. D., Rizzo, C. J., and Harris, T. H. (2004) Coupling products of nucleosides with the glyoxal adduct of deoxyguanosine, *Chem. Res. Toxicol. 17*, 1047−1056.

(33) Loeppky, R. N., Cui, W., Goelzer, P., Park, and Ye, Q. (1999) Glyoxal-guanine DNA adducts: detection, stability and formation in vivo from nitrosamines, *IARC Sci. Pub. 150*, 155−168.

(34) Fraenkel-Konrat, H. (1954) Reaction of nucleic acid with formaldehyde, *Biochim. Biophys. Acta 15*, 307−309.

(35) Staehlin, M. (1958) Reaction of tobacco mosaic virus nucleic acid with formaldehyde, *Biochim. Biophys. Acta 29*, 410−417.

(36) Grossman, L., Levine, S. S., and Allison, W. S. (1961), The reaction of formaldehyde with nucleotides and T2 bacteriophage DNA, *J. Mol. Biol. 3*, 47−60.

(37) Munter, T., Cottrell, L., Hill, S., Kronberg, L., Watson, W. P., and Golding, B. T. (2002) Identification of adducts derived from reactions of (1-chloroethenyl)oxirane with nucleoside and calf thymus DNA, *Chem. Res. Toxicol. 15*, 1549−1560.

(38) Pluskota-Karwatka, D., Le Curieux, F., Munter, T., Sjöholm, R., and Kronberg, L. (2002) Identification of conjugate adducts formed in the reactions of malonaldehyde-acetaldehyde and malonaldehyde-formaldehyde with cytidine, *Chem. Res. Toxicol. 15*, 110−117.

(39) Kronberg, L., Asplund, D., Maki, J., and Sjöholm, R. (1996) Reaction of mucochloric and mucobromic acids with adenosine and cytidine: Formation of chloro- and bromopropenal derivatives, *Chem. Res. Toxicol. 9*, 1237−1263.

(40) Kronberg, L., Karlsson, S., and Sjöholm, R. (1993) Formation of ethenocarbaldehyde derivatives of adenosine and cytidine in reactions with mucochloric acid, *Chem. Res. Toxicol. 6*, 495−499.

(41) Stone, K., Uzieblo, A., and Marnett, L. J. (1990) Studies of the reaction of malondialdehyde with cytidine nucleosides, *Chem. Res. Toxicol. 3*, 467−472.

TX0496688